Isolation methods commonly used to study the liposomal protein corona suffer from contamination issues

Kristensen, Kasper; Münter, Rasmus; Kempen, Paul J.; Thomsen, Mikkel E.; Stensballe, Allan; Andresen, Thomas L.

Published in:
Acta Biomaterialia

Link to article, DOI:
10.1016/j.actbio.2021.06.008

Publication date:
2021

Document Version
Peer reviewed version

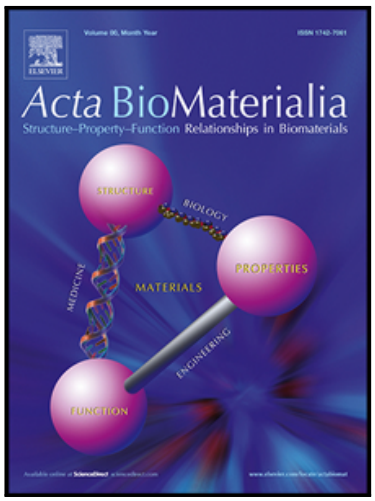

Isolation methods commonly used to study the liposomal protein corona suffer from contamination issues

Kasper Kristensen , Rasmus Münter , Paul J. Kempen , Mikkel E. Thomsen , Allan Stensballe , Thomas L. Andresen

PII: S1742-7061(21)00375-5
DOI: https://doi.org/10.1016/j.actbio.2021.06.008
Reference: ACTBIO 7422

To appear in: *Acta Biomaterialia*

Received date: 15 December 2020
Revised date: 26 May 2021
Accepted date: 1 June 2021

Please cite this article as: Kasper Kristensen , Rasmus Münter , Paul J. Kempen , Mikkel E. Thomsen , Allan Stensballe , Thomas L. Andresen , Isolation methods commonly used to study the liposomal protein corona suffer from contamination issues, *Acta Biomaterialia* (2021), doi: https://doi.org/10.1016/j.actbio.2021.06.008

Isolation methods commonly used to study the liposomal protein corona suffer from contamination issues

Kasper Kristensen[1,*], Rasmus Münter[1], Paul J. Kempen[1], Mikkel E. Thomsen[2], Allan Stensballe[2], and Thomas L. Andresen[1,*]

[1]DTU Health Tech, Department of Health Technology, Technical University of Denmark, 2800 Kgs. Lyngby, Denmark, [2]Department of Health Science and Technology, Aalborg University, 9220 Aalborg Ø, Denmark

*Corresponding author. E-mail addresses: kakri@dtu.dk (K. Kristensen), tlan@dtu.dk (T.L. Andresen)

Abstract

The liposomal protein corona has been the focus of numerous studies, but there is still no consensus regarding its extent and composition. Rather, the literature is full of conflicting reports on the matter. To elucidate whether there could be a methodological explanation for this, we here scrutinize the efficiency of three commonly used liposome isolation methods at isolating stealth liposomes from human plasma. Firstly, we show that size-exclusion chromatography (SEC) in its standard form is prone to isolating unbound protein material together with the liposomes, but also that the method may be optimized to mitigate this issue. Secondly, we demonstrate that SEC in combination with membrane ultrafiltration is no better at removing the unbound protein material than SEC alone. Thirdly, we show that centrifugation is not able to pellet the liposomes. Overall, our results suggest that previous research on the liposomal protein corona may have suffered from significant methodological problems, in particular related to contaminant proteins interfering with the analysis of the protein corona. We believe that the data presented here may help guide future research around this challenge to reach a converging understanding about the properties of the protein corona on liposomes.

Keywords

Protein corona; liposomes; isolation methods; size-exclusion chromatography; membrane ultrafiltration

Graphical abstract

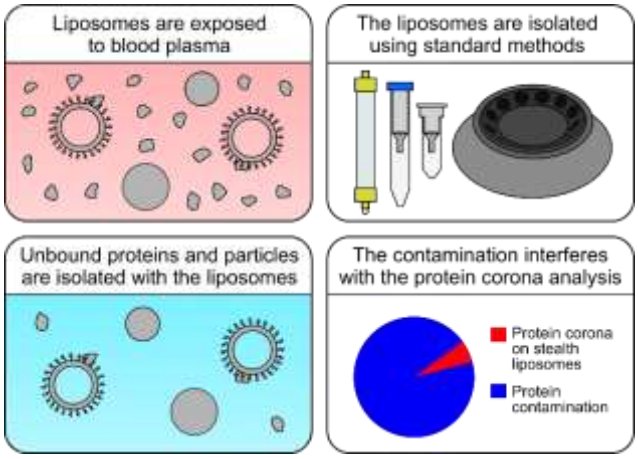

Statement of significance

Upon administration into the circulatory system, liposomal drug carriers encounter an environment rich in proteins. These proteins may adsorb to the liposomes to form what is known as the protein corona, potentially governing the interactions of the liposomes with tissues and cells. However, despite decades of intense research efforts, there is currently no clear understanding about the extent and composition of the liposomal protein corona, making it impossible to assess its mechanistic importance. Here we report that the methods commonly used to isolate liposomes from blood plasma or serum to study the protein corona are susceptible to protein contamination. This may be the underlying technical reason for the current confusion about the characteristics of the liposomal protein corona.

1. Introduction

Liposomes represent one of the most commonly used type of drug nanocarrier. Based on biocompatible constituents, they can be engineered to carry a variety of different drugs, ensuring local accumulation of the drugs at specific tissues or even inside targeted cells [1]. Testifying to the potential of liposomes, there are already numerous liposomal drug formulations available in the clinic, and likely more on the way [2]. However, to design a next, improved generation of liposome-based formulations, a better understanding of the mechanisms governing the behavior of liposomes in physiological environments is required [3].

Upon their introduction into the circulatory system, liposomes are subject to a series of complex interactions that essentially determine their fate. To unravel these interactions, particular emphasis is often put on the concept of the protein corona [4]. According to this concept, plasma proteins will bind to the liposomes to alter their surface properties and, thereby, govern their circulation longevity, biodistribution, targeting ability, and propensity for adverse reactions [5,6].

In spite of the mechanistic significance placed on the liposomal protein corona, its characteristics are not well understood. The best illustration of this is the variation of the protein binding value (defined as the g protein bound per mol lipid [7,8]) reported for liposomes isolated upon exposure to serum or plasma. For instance, reports on the protein binding value vary in the range of ∼10-200 g protein per mol lipid for liposomes consisting of saturated phosphatidylcholine and cholesterol [8-12] and in the range of ∼20-200 g protein per mol lipid for similar liposomes based on unsaturated rather than saturated phosphatidylcholine [7,13]. The most prominent example to bring forward in this context, however, is that of the classic PEGylated stealth liposomes consisting of saturated phosphatidylcholine, cholesterol and PEGylated saturated phosphatidylethanolamine: For this type of liposome, the protein binding value has been reported to be everywhere from <10 to >1000 g protein per mol lipid [8,10-12,14-17]; in other words, the reported values span more than two orders of magnitude, thereby describing protein coronas of vastly different extents.

The confusion about the protein corona on stealth liposomes recently prompted us to perform a comprehensive study [18]. The results of that study unambiguously demonstrated the protein corona on stealth liposomes to be sparse, the protein binding value estimated to be similar to or maybe even lower than the lowest values cited above. Disseminating our work, we mainly focused on this finding, but we also mentioned another equally important finding, namely that size-exclusion chromatography (SEC)–which is a commonly used method for isolating liposomes from serum and plasma [10,11,14]–is prone to protein contamination, that is, unbound serum and plasma proteins co-elute with the liposomes. Even though this issue represents an obvious methodological challenge for studies on the liposomal protein corona, it has so far not received much attention. The aim of the

present study was, therefore, to bring the contamination issue to the center of the stage. Focusing on SEC as a method for isolating stealth liposomes, we investigated the contamination from human plasma prepared with different anticoagulants and centrifugation protocols. We found that SEC in its standard form is highly susceptible to protein contamination, but also that the contamination may be greatly reduced by optimizing the plasma preparation procedure and increasing the length of the SEC column. On the other hand, combining SEC with membrane ultrafiltration–as is commonly done [12,13,15-17,19-21]–was found not to mitigate the contamination issue. For completeness, we also wanted to investigate the contamination when isolating stealth liposomes using centrifugation, but we found that this method was unable to pellet the liposomes, preventing us from doing any further experiments.

Overall, our work revealed several critical shortcomings of the current standard liposome isolation methods, in particular related to the issue of protein contamination. If not taken properly into account, the contamination may interfere with the analysis of the protein corona, causing researchers to draw erroneous conclusions. This strongly implies that all studies on the liposomal protein corona should include a control experiment to evaluate the efficiency of the chosen liposome isolation method. Going through the literature, however, it seems that such a control experiments are rarely performed, representing a potential explanation for the widespread confusion about the nature of the liposomal protein corona.

2. Materials and Methods

Many of the experimental protocols used in the present study are similar to that of our previous work [18], albeit with some modifications.

2.1. Materials

1,2-Distearoyl-*sn*-glycero-3-phosphocholine (DSPC), ovine cholesterol, and 1,2-distearoyl-*sn*-glycero-3-phosphoethanolamine-N-[methoxy(polyethylene glycol)-2000] ammonium salt (DSPE-PEG2k) were purchased from Avanti Polar Lipids (Alabaster, AL, USA). 1,2-Dipalmitoyl-*sn*-glycero-3-phosphoethanolamine labeled with Atto 488 (Atto 488 DPPE) was purchased from Atto-Tec (Siegen, Germany). *tert*-Butanol was purchased from VWR Chemicals (Radnor, PA, USA). Vacutainer blood collections tubes in plastic coated with dipotassium ethylenediaminetetraacetic acid (EDTA, dimensions 16×100 mm, volume 10 mL) or lithium heparin (dimensions 16×100 mm, volume 10 mL), or containing 129 mM sodium citrate solution (dimensions 13×75 mm, volume 2.7 mL) were purchased from BD (Franklin Lakes, NJ, USA). 4-(2-Hydroxyethyl(piperazine-1-ethanesulfonic acid (HEPES), sodium chloride (NaCl), sodium hydroxide (NaOH), phosphorus standard for inductively coupled plasma (ICP), sodium deoxycholate, triethylammonium bicarbonate, tris(2-carboxyethyl)phosphine, 2-chloroacetamide, ethyl acetate, and MS Qual/Quant QC mix were purchased from Sigma-Aldrich (St. Louis, MO, USA). Micro-BCA and Pierce coomassie plus (Bradford) proteins assay kits, Pierce trypsin protease MS grade, trifluoroacetic acid, acetonitrile, and formic acid acid were purchased from Thermo Fisher Scientific (Waltham, MA, USA). Slurry for preparing Sepharose CL-4B columns was purchased from GE Healthcare (Little Chalfont, UK). Econo-Column glass chromatography columns (dimensions 1.5×20 and 1.5×50 cm) was purchased from Bio-Rad (Hercules, CA, USA). Protein LoBind tubes were purchased from Eppendorf (Hamburg, Germany).

2.2. Liposome preparation and characterization

DSPC, cholesterol, DSPE-PEG2k, and Atto 488 DPPE (molar ratio 56.2:38.2:5.5:0.1) were dissolved in tert-butanol/Milli-Q water (9:1). To ensure complete dissolution of the lipids, the solutions were heated to ~40-50 °C. Subsequently, the solutions were plunge-frozen in liquid nitrogen and lyophilized overnight to remove the solvent.

HEPES buffer (10 mM HEPES, 150 mM NaCl, pH 7.4) was added to the lipid mixtures to obtain a lipid concentration of 50 mM. The lipid suspensions were subject to gentle vortexing every 5 min for a total period of 30 min, and then extruded 21 times through a 100-nm polycarbonate filter (Whatman, GE Healthcare) using a mini-extruder (Avanti Polar Lipids) to form liposomes. Throughout the entire hydration and extrusion process, the lipid samples were heated to at least 65 °C.

To determine their phospholipid concentration, the prepared liposome stock samples were diluted ×8400 in 2% HCl, 10 ppb Ga aqueous solution and evaluated using inductively coupled plasma mass spectrometry (ICP-MS, done on an iCAP Q ICP-MS, Thermo Fisher Scientific) by comparing to a set of standard phosphorus samples in the range 0-100 ppb. Since cholesterol does not contain phosphorus, the total lipid concentration of the liposome stock samples was determined by dividing the measured phospholipid concentrations with 0.618.

To determine their size, the liposomes were diluted to 100 µM and 25 nM (concentration in terms of lipid) in HEPES buffer and evaluated using DLS and NTA, respectively.

2.3. Plasma preparation

Blood was drawn by certified staff from human donors. Following the guidelines of the National Committee on Health Research Ethics, all donors had given signed consent, and their identities were unknown to the researchers involved in the study. While still in the collection tube, the blood was centrifuged for 15 min at 2000 × *g* at 4 °C. The plasma supernatant was transferred to a 15-mL Protein LoBind tube, which was gently inverted a few times to ensure complete mixing of the plasma. The plasma was then either (i) transferred in 810-µL aliquots to 1.5-mL or 2-mL Protein LoBind tubes and used for the experiments described below or (ii) transferred in 900-µL aliquots to 1.5-mL Protein LoBind tubes and subject to extended centrifugation for 30 min at 12,100 × *g* at room temperature before transferring 810 µL of the supernatant in each tube to a 2-mL Protein LoBind tube and using it for the experiments described below.

2.4. Sample preparation and incubation

To prepare plasma samples with liposomes, liposome stock samples and HEPES buffer was added to 810 µL plasma in 1.5-mL Protein LoBind tubes (for centrifugation isolation experiments) or 2-mL Protein LoBind tubes (for SEC isolation experiments) to obtain a final lipid concentration of 2 mM (concentration in terms of lipid) and a final sample volume of 900 µL. To prepare corresponding blank samples, 90 µL HEPES buffer without liposomes was added to 810 µL plasma. All samples were incubated for 1 h at 37 °C in a PHMT-PSC18 thermoshaker (Grant Instruments, Cambridge, UK) at 500 rpm before being used for the experiments described below.

2.5. Size-exclusion chromatography (SEC)

After incubation, 500 µL of each plasma sample was loaded onto a Sepharose CL-4B column (dimensions 1.5×20 cm) and eluted with HEPES buffer at a flow rate of 1 mL min^{-1}. Column fractions of 1 min were collected in 2-mL Protein LoBind tubes. DLS, NTA, TEM and LC-MS/MS analyses of the

void-volume fractions were done by pooling fractions 8-11. The same fractions were also pooled for the membrane ultrafiltration protocol described below.

For a few experiments, the plasma was loaded onto a longer Sepharose CL-4B column (dimensions 1.5×50 cm) and eluted with HEPES buffer at a flow rate of 0.5 mL min^{-1}. For these experiments, column fractions of 2 min were collected in 2-mL Protein LoBind tubes.

2.6. Membrane ultrafiltration

The membrane ultrafiltration protocol was similar to an already published protocol [12]: 2 mL of the pooled SEC void-volume fractions was loaded onto a Vivaspin 6 centrifugal filter unit (10,000 MWCO; Sartorius, Göttingen, Germany) and concentrated to ~500 µL by centrifuging at 2000 × *g*. The concentrated sample was transferred to a Vivaspin 500 centrifugal filter unit (1,000,000 MWCO; Satorius) and further concentrated to ~100 µL by centrifuging at 2000 × *g*. Three consecutive washing steps of the concentrated sample was then performed, each time adding 100 µL HEPES buffer and centrifuging at 2000 × *g* until the sample volume in the filter unit was back at ~100 µL.

To test whether control experiments with blank plasma provided an accurate representation of the contamination recovered from plasma with liposomes, the pooled void-volume fractions of SEC runs with blank plasma were supplemented with 250 µM liposome (concentration in terms of lipid) to obtain a similar liposome concentration to that of the pooled void-volume fractions of SEC runs with plasma containing liposomes. The samples were then treated with the above membrane ultrafiltration protocol.

2.7. Centrifugation

After incubation, the tubes with the plasma samples were transferred to a 5417C centrifuge (Eppendorf) and centrifuged at 17,900 × *g* for 30 min at room temperature. The supernatant was then removed from the tubes for further analysis.

2.8. Micro bicinchoninic acid (micro-BCA) assay

150 µL of each sample under investigation was transferred to a 2-mL Protein LoBind tube. Then, 150 µL working reagent was added to all tubes. The tubes were subsequently incubated for 1 h in a 60 °C water bath. Upon cooling at room temperature for a few minutes, 250 µL of each sample was then transferred to a transparent 96-well microplate, and the absorbance measured at 562 nm using a Spark multimode microplate reader (Tecan, Männedorf, Switzerland). The protein mass concentration of each sample was estimated by comparing its measured absorbance to those of a set of bovine serum albumin standard samples in the range 0-100 µg mL^{-1}. Samples with a protein mass concentration >100 µg mL^{-1} were appropriately diluted in HEPES buffer before investigation. The liposomes gave a small contribution to the measured absorbances, so the measured protein concentrations were corrected by the equation

$$c_{\mathrm{cor}} = c_{\mathrm{meas}} - K_{\mathrm{lip}} C_{\mathrm{lip}}, \quad (1)$$

where c_{cor} is the corrected protein mass concentration, c_{meas} is the measured protein mass concentration, C_{lip} is the molar lipid concentration, and K_{lip} is the magnitude of the liposome contribution to the micro-BCA assay. The value of K_{lip} was determined in a separate experiment for each batch of liposomes and was always found to be ~2 µg mL^{-1} mM^{-1}.

2.9. Bradford assay

125 µL of each sample under investigation was transferred to a transparent 96-well microplate. Then, 125 µL Bradford reagent was added to all wells. The 96-well plate was incubated for 10 min at room temperature, and subsequently, the absorbances at 595 nm was measured using a Spark multimode microplate reader. The protein mass concentration of each sample was estimated by comparing its measured absorbance to those of a set of bovine serum albumin standard samples in the range 0-100 µg mL^{-1}. Samples with a protein mass concentration >100 µg mL^{-1} were appropriately diluted in HEPES buffer before investigation. The measured protein concentrations were corrected for the liposome contribution using Equation 1, and K_{lip} was determined for each liposome batch, in all cases found to be ~2-4 µg mL^{-1} mM^{-1}.

2.10. Lipid quantification by fluorescence

150 µL of each sample under investigation, usually diluted ×4-10 in HEPES buffer, was transferred to a black 96-well microplate. The fluorescence intensity of the samples was measured using a Spark multimode microplate reader with an excitation wavelength of 502 nm and an emission wavelength of 525 nm. The lipid concentration of each sample was estimated by comparing its fluorescence intensity to that of a standard liposome sample with 100 µM lipid, assuming the intensity to be linearly proportional to the lipid concentration.

2.11. Dynamic light scattering (DLS)

~100 µL of each sample under investigation was transferred to a UV cuvette (window 2 mm × 3.5 mm, path length 1 cm; Brand, Wertheim, Germany). DLS was performed using a Zetasizer Nano ZS (Malvern,Worcestershire, UK). The acquired data were analyzed using both cumulant and size distribution analysis.

2.12. Nanoparticle tracking analysis (NTA)

The samples under investigation were diluted to ~25 nM liposome (concentration in terms of lipid) in HEPES buffer. NTA was performed using a ZetaView PMX-120 BASIC microscope (Particle Metrix, Meerbusch, Germany) in fluorescence mode. The excitation source was a 488-nm laser, and the fluorescence emission was detected after passing a 500-nm long wave-pass cut-off filter.

2.13. Transmission electron microscopy (TEM)

3 µl of each sample under investigation was applied to freshly glow discharged 200 mesh nickel TEM grids coated with a carbon stabilized formvar film (FCF200-Ni, Electron Microscopy Sciences, Hatfield, PA, USA). The solutions were allowed to adsorb for 4 min after which the grids were rinsed three times on droplets of Milli-Q water before being stained with 2% uranyl acetate. The grids were sequentially placed on droplets of 2% uranyl acetate for 10 sec, 2 sec, and 20 sec. Excess uranyl acetate solution was wicked away using a piece of filter paper placed perpendicular to the grid surface, and the grids were allowed to dry overnight before analysis. TEM was performed utilizing a FEI Tecnai T12 Biotwin TEM (Thermo Fisher Scientific) operating at 120 kV located at the Center for Electron Nanoscopy at the Technical University of Denmark, and images were acquired using a bottom-mounted charge-coupled device camera (Orius SC1000WC, Gatan, California, USA)

2.14. Liquid chromatography-tandem mass spectrometry (LC-MS/MS)

250 µL of each sample under investigation was mixed with 250 µL lysis buffer (5% sodium deoxycholate, 50 mM triethylammonium bicarbonate, pH 8.5) in 1.5-mL Protein LoBind tubes. To denature the proteins, the samples were incubated for 5 min at 95 °C. The samples were then transferred to a Microcon-10 kDa centrifugal filter unit (Merck, Darmstadt, Germany) and centrifuged at 14,000 × *g* until the solvent had flown through the filter. After discarding the filtrate, the samples were reduced and alkylated by adding 200 µL 10 mM tris(2-carboxyethyl)phosphine, 50 mM 2-chloroacetamide in digestion buffer (0.5% sodium deoxycholate, 50 mM triethylammonium bicarbonate, pH 8.5) and incubated for 30 min at 37 °C. The samples were then centrifuged again at 14,000 × *g* until the solvent had flown through the filter. The filtrate was discarded. To wash the samples, 200 µL digestion buffer was then added, and the samples were again centrifuged at 14,000 × *g* until the solvent had flown through the filter. The inner spin filters with the samples were subsequently transferred to new collection tubes, and 50 µL 20 µg mL^{-1} Pierce trypsin protease in digestion buffer was added. The samples were incubated overnight at 37 °C to digest the proteins. The next day, the samples were centrifuged at 14,000 × *g* until the protein digest had flown through the filters into the collection tubes. To ensure complete recovery of the protein digest, 100 µL 50 mM triethylammonium bicarbonate, pH 8.5 buffer was added to the filters, which were then again centrifuged at 14,000 × *g* until the buffer had flown through the filters and into the collection tubes. Next, the inner spin filters were discarded, and 450 µL ethyl acetate and 7.5 µL trifluoroacetic acid was added to all tubes. The tubes were vortexed and centrifuged at 14,000 × *g* for 5 min to obtain phase separation. The top phase contained the sodium deoxycholate, whereas the bottom phase contained the peptides. The top phase was removed by pipette to remove the sodium deoxycholate. An additional volume of 450 µL ethyl acetate was added to all samples, which were then again vortexed and centrifuged at 14,000 × *g* for 5 min to obtain phase separation again. The top phase was removed by pipette to ensure complete removal of sodium deoxycholate. Each sample was dried in a Concentrator Plus vacuum centrifuge (Eppendorf) and resuspended in 30 µL 2% acetonitrile, 0.1% trifluoroacetic acid, 0.1% formic acid aqueous solution. The samples were vortexed, spun down using a minicentrifuge, and ultrasonicated for 2 min. Subsequently, the samples were spun down at 14,000 × *g*, and 8 µL of the supernatant was loaded into a 96-well microplate and spiked with 2 µL MS Qual/Quant QC Mix, yielding a total volume of 10 µL, which was all injected. The samples were investigated using a UPLC-nanoESI MS/MS setup consisting of a Dionex RSLC nanopump (Dionex RSLC 3500, Thermo Fisher Scientific) connected to a Q Exactive HF-X-Hybrid Quadrupole-Orbitrap mass spectrometer (Thermo Fisher Scientific). The peptide samples were loaded onto a C18 reversed-phase pre-column (Dionex Acclaim PepMap RSLC C18, 2 µm, 100 Å, 100 µm × 2 cm) and separated on a 50-cm analytical C18 Micro pillar array column (µPAC, PharmaFluidics, Gent, Belgium) at 30 °C with a constant flow rate of 0.75 µL/min. The mobile phases were (A) water with 2% acetonitrile and 0.1% formic acid and (B) acetonitrile with 0.1% formic acid. The loading was done with 2% B over 5 min. The separation was performed by a linear gradient from 8% B to 30% B over 35 min. A full MS scan in the mass range of m/z 375 to 1200 was acquired at a resolution of 120,000. The precursor ions were isolated using a quadrupole isolation window of m/z 1.6 and fragmented using higher-energy collision dissociation (HCD) with a normalised collision energy of 28. Fragmented ions were dynamically added to an exclusion list for 15 s. All acquired MS scans were searched using default settings in MaxQuant/Andromeda 1.6.10.43 [22] against a human core reference database (Uniprot UP000005640, proteins entries: 20.368, accessed 20/10-2019). Standard settings were employed with carbamidomethyl (C) as a static modification, and protein N-

terminal acetylation, deamidation (NQ) and oxidation (M) as variable modifications. Protein identification was reported at a false detection rate of 1%, with identification match between runs toggled on. The MaxQuant results were processed using Perseus 1.6.10.43 [23]. One or more unique peptides were required for protein identification. Proteins only identified by site and reverse peptides were removed from the results. Keratins were considered to be contaminants and were also removed from the final list of proteins.

2.15. Statistical analysis

Data are generally presented as mean ± standard deviation, except for representative example data from individual experiments.

3. Results and Discussion

3.1. Preparation and characterization of liposomes

The experiments to be described in the following sections were based on PEGylated stealth liposomes, prepared by the standard extrusion method [1]. To allow for their easy detection, the liposomes incorporated the fluorescently labeled lipid Atto 488 DPPE. Using dynamic light scattering (DLS) and fluorescence-mode nanoparticle tracking analysis (NTA), the liposomes were determined to have a size of ~120-140 nm with a narrow size distribution, see Figure S1 in the Supplementary material.

3.2. Isolation of liposomes using size-exclusion chromatography (SEC)

The SEC gel material most commonly used for isolation of liposomes from serum or plasma is Sepharose CL-4B [10-13,15-21]. On paper, this makes sense: Compared to other gel materials, Sepharose CL-4B has a high protein exclusion limit of 20,000 kDa, roughly corresponding to a size exclusion limit of 42 nm [24]. This means that liposomes–which typically are of a size of ~100 nm–are expected to pass straight through the gel material whereas even large plasma particles are expected to be retained.

To evaluate the ability of Sepharose CL-4B to isolate liposomes from plasma, we incubated 2 mM stealth liposomes (concentration in terms of lipid) with human EDTA plasma for 1 h at 37 °C under constant shaking. We then loaded 500 µL of the samples onto a 1.5×20-cm Sepharose CL-4B column. By this procedure, the liposome concentration, sample volume and column dimensions were similar to those typically used in other studies [11-17,19-21]. For reference, we also included blank plasma samples in our study. The elution of the plasma proteins was probed using both the micro-BCA and Bradford protein assays, and the elution of the liposomes was probed using the fluorescence from Atto 488, assuming linear proportionality between the liposome concentration and the fluorescence emission intensity (this assumption is verified in Figure S2 in the Supplementary material). At first glance, the recorded elution profiles, shown in Figure S3 in the Supplementary material, demonstrated good separation between the liposomes and the unbound plasma proteins, but zooming in on the void volume, as done in Figures 1A,B and S4 in the Supplementary material, shows that the situation was not as simple as that. Some protein eluted together with the liposomes in the void volume, and at the same time–even though the Bradford assay determined a lower amount of protein than the micro-BCA assay–the protein elution profile for each of the two protein assays was similar for plasma with and without liposomes. The only possible interpretation of this is that contaminant proteins were co-eluting with the liposomes, and that these proteins were far more

abundant than the proteins in the corona [18,25]. If we wanted to study the protein corona of the liposomes, the contaminant proteins would thus represent a severe limitation. However, the aim of our work was not to study the protein corona, but rather to study the contamination itself. From that perspective, the stealth liposomes provided a suitable model system, allowing us to study the protein contamination co-eluting with the liposomes without any significant interference by corona proteins.

Based on the collected elution profiles, we next wanted to proceed with a rigorous analysis of the ability of the Sepharose CL-4B column to isolate the liposomes. The most basic requirement of any liposome isolation method is that it is able to recover the liposomes, so to evaluate whether the Sepharose CL-4B column fulfilled this requirement, we did two things. Firstly, we calculated the amount of lipid eluting in the void volume from plasma with liposomes, see Figure 1C. The lipid in

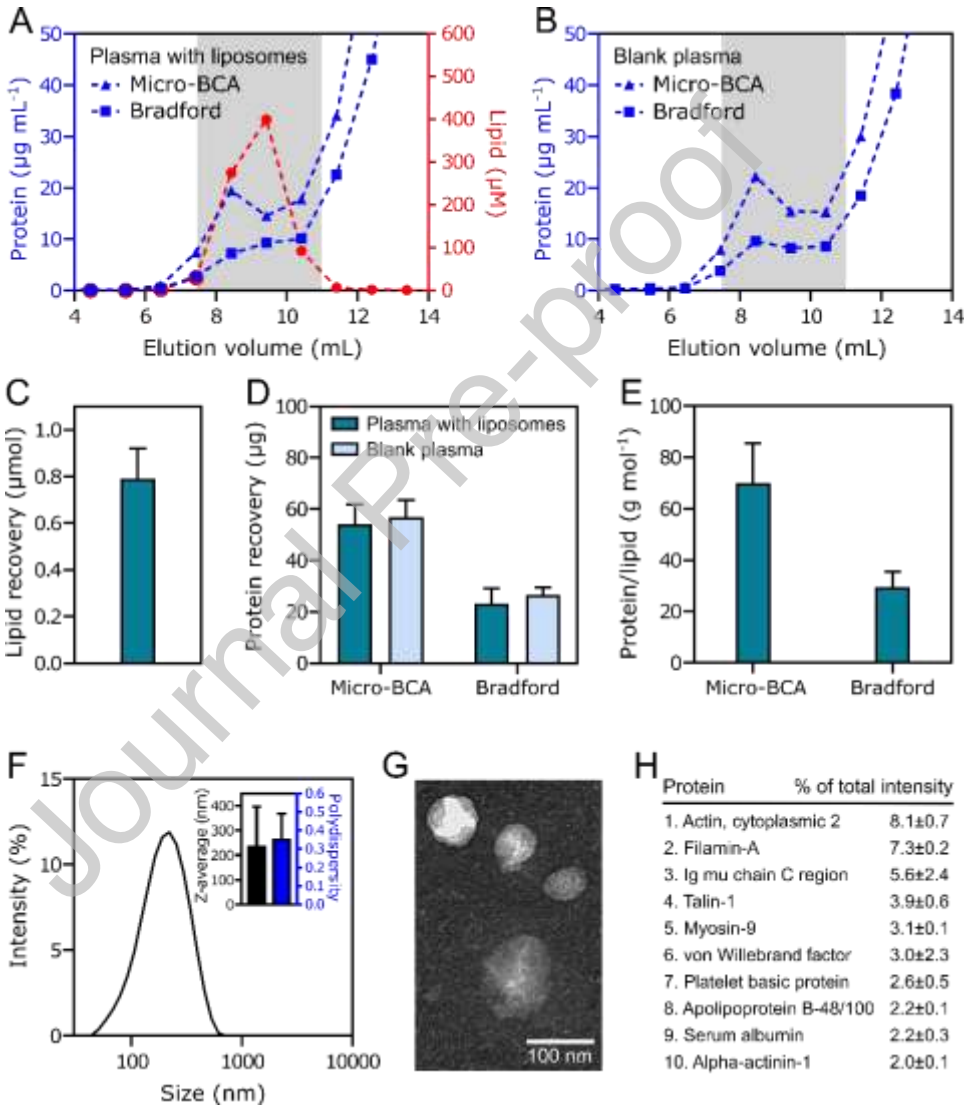

Figure 1. Experiment with EDTA plasma run on a 1.5×20-cm Sepharose CL-4B column. (A,B) Elution profiles in the vicinity of the void volume for plasma incubated with liposomes (A) or without liposomes (B). The shaded areas show the void volume. (C) Lipid recovered in the void volume for plasma incubated with liposomes. (D) Protein recovered in the void volume for both plasma incubated with or without liposomes. (E) Protein-to-lipid ratio in the void volume for plasma incubated with liposomes. (F) Contaminant particle size distribution, determined using DLS. The insert shows the cumulant analysis results. (G) TEM image of contaminant particles. (H) The ten most abundant contaminant proteins identified using LC-MS/MS. Panels A, B, F (excluding the insert), and G show example data from one sample; Panels C-E show the average data of five separate samples; Panel F (insert only) shows the average data of three separate samples; and Panel H shows the average data of two separate samples. The error bars/experimental uncertainties represent the

the void volume represented ~80% of the lipid loaded onto the column, that is, most of the lipid loaded onto the column was recovered in the void volume. Secondly, we used fluorescence-mode NTA to confirm that the lipid eluting in the void volume represented intact liposomes, see Figure S5 in the Supplementary material. Thus, it is clear that the majority of the liposomes loaded onto the column eluted in the void volume, and incidentally, that the Atto 488 label remained associated with the liposomes during 1 h incubation in plasma, in agreement with our previous observations [18,26].

Having confirmed that the Sepharose CL-4B column can be used to recover the liposomes from plasma, we next calculated the amount of protein in the void volume for plasma incubated both with and without liposomes, see Figure 1D. Doing this, we arrived at the same conclusions that we did from the visual inspection of the elution profiles: The amount of protein in the void volume was similar in the absence and presence of the liposomes, and also, the Bradford assay only measured 45±7% of the protein determined by the micro-BCA assay. One additional important point, however, also followed from the calculation: The contaminant protein in the void volume only represented ~0.1% of the total amount of protein loaded onto the column. In other words, the Sepharose CL-4B column almost completely separated the liposomes from the plasma proteins, but the miniscule amount of contaminant protein that remained in the void volume completely masked the putative protein corona.

To put our results further into perspective, we calculated the protein-to-lipid ratio in the void volume for the experiments with plasma incubated with liposomes, see Figure 1E. Importantly, the calculated ratio was similar to that reported in several other studies using SEC to isolate stealth liposomes [11,14], except that in those studies, the protein-to-lipid ratio was taken to represent the protein binding value. It is thus evident that protein contamination may severely bias the results for stealth liposomes when using a Sepharose CL-4B column to isolate the liposomes.

With the potential impact of the contamination in mind, we next thought it pertinent to characterize its nature. Therefore, we investigated the void-volume eluate blank plasma using DLS. The results of this, shown in Figure 1F, demonstrate that the contamination contained a polydisperse collection of particles in the size range 50-500 nm. To further corroborate this observation, we also investigated the void-volume eluate of blank plasma using transmission electron microscopy (TEM). The acquired images confirm that the contamination contained particles of approximately the size indicated by DLS, see Figure 1G. Underscoring that these particles were specific to plasma, we found that the void-volume eluate of a blank buffer sample neither yielded a DLS signal above the background level nor any detectable particles in TEM (data not shown).

From a theoretical point of view, plasma may contain several components of similar size to the liposomes, for example, lipoproteins, extracellular vesicles, and various protein aggregates [27]. To reveal whether any of these components were part of the contamination, we used liquid chromatography-tandem mass spectrometry (LC-MS/MS) to identify the proteomic content of the void-volume eluate of blank plasma, see Figure 1H. This analysis revealed that many of the most abundant contaminant proteins were known to be associated with the cytoskeleton (actin, cytoplasmic 2; filamin-A; talin-1; myosin-9; alpha-actinin-1), indicating that much of the contamination either was made up of cellular debris or, alternatively, extracellular vesicles [28]. Incidentally, it should be mentioned that the proteomic content was similar for the plasma samples containing liposomes (see Figure S6A in the Supplementary material), meaning that the protein corona on the investigated liposomes was so sparse that it was not even detectable by LC-MS/MS, even though this is a very sensitive technique.

The above experiments were performed using plasma prepared with EDTA, since this anticoagulant is commonly used in studies on the liposomal protein corona [12,15-20,29-31], but studies on the protein corona on other nanomaterials often use citrate as the anticoagulant [32-34]. To investigate whether protein contamination was also an issue for plasma prepared with citrate, we next redid the above experiments using this anticoagulant instead of EDTA. Examples of the elution profiles recorded in the experiments with citrate plasma are shown in Figures 2A,B and S7 in the Supplementary material. Compared to the EDTA plasma elution profiles, there was significantly more inter-donor variability for the citrate plasma elution profiles, but for each individual donor, the elution profiles again appeared largely similar with and without liposomes, demonstrating that contamination was also an issue for the citrate plasma. Further corroborating this point, the amount of lipid and protein eluting in the void volume for the citrate plasma were comparable to the

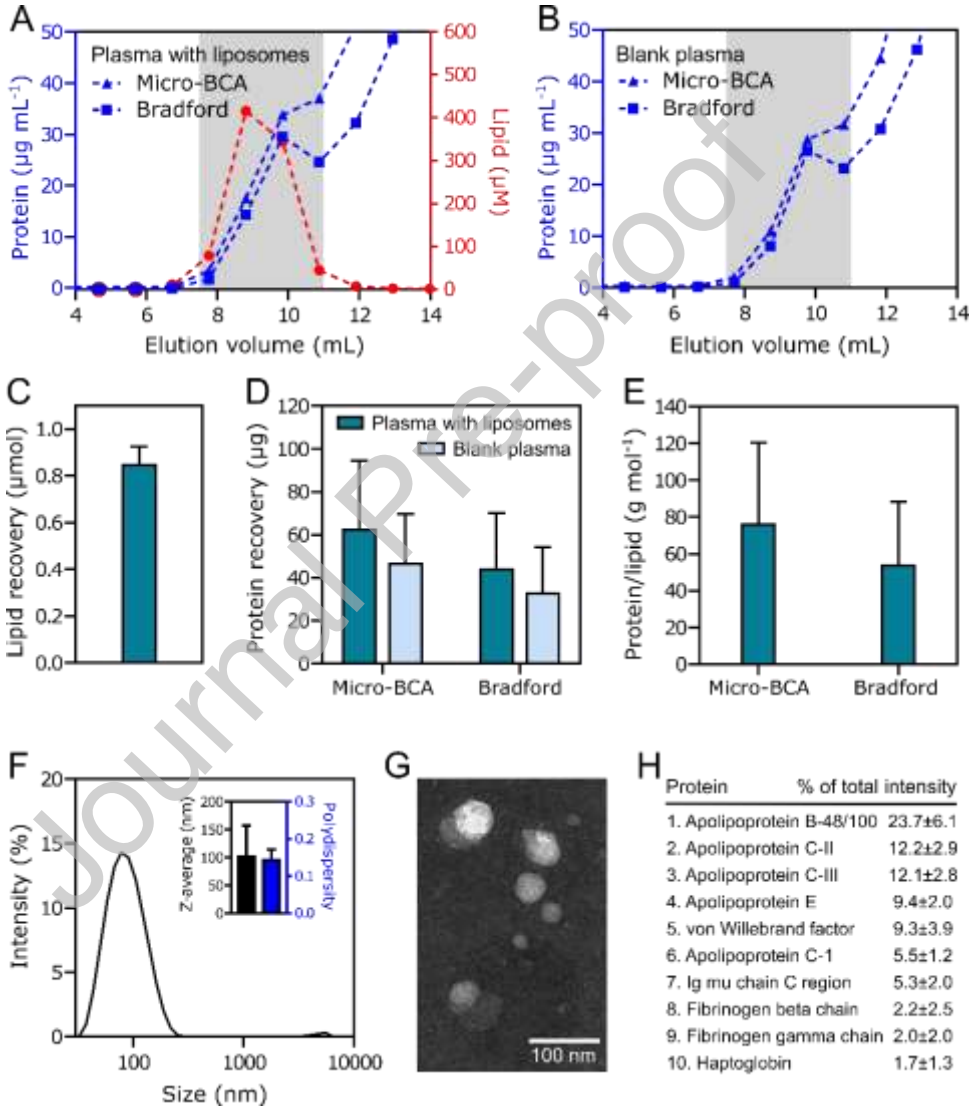

Figure 2. Experiment with citrate plasma run on a 1.5×20-cm Sepharose CL-4B column. (A,B) Elution profiles in the vicinity of the void volume for plasma incubated with liposomes (A) or without liposomes (B). The shaded areas show the void volume. (C) Lipid recovered in the void volume for plasma incubated with liposomes. (D) Protein recovered in the void volume for both plasma incubated with or without liposomes. (E) Protein-to-lipid ratio in the void volume for plasma incubated with liposomes. (F) Contaminant particle size distribution, determined using DLS. The insert shows the cumulant analysis results. (G) TEM image of contaminant particles. (H) The ten most abundant contaminant identified using LC-MS/MS. Panels A, B, F (excluding the insert), and G show example data from one sample; Panels C-E show the average data of four separate samples; and Panels F (insert only) and H show the average data of three separate samples. The error bars/experimental uncertainties represent the standard deviation.

amounts eluting in the void volume for the EDTA plasma, see Figure 2C-E; that is, also for the citrate plasma, the protein contamination led to a fairly high protein-to-lipid ratio in the void volume. Despite the contamination issue being of an overall similar magnitude, though, a close examination of the protein recovered in the void volume revealed two differences between the experiments with the citrate and EDTA plasma that are worth highlighting: Firstly, normalizing the amount of protein eluting in the void volume for plasma with liposomes to the amount of protein eluting in the void volume for plasma from the same donor without liposomes, as done in Figure S8 in the Supplementary material, confirmed that a similar amount of protein was recovered with and without liposomes in the experiments with the EDTA plasma, but also demonstrated that ~40% more protein was recovered with the liposomes than without the liposomes in the experiments with the citrate plasma. This could be taken to indicate the existence of a protein corona on the liposomes in the citrate plasma, but as discussed below, this interpretation may not be correct. Secondly, in the experiments with the citrate plasma, the Bradford assay measured 65±11% of the protein determined by the micro-BCA assay. As mentioned before, the same value was ~45% in the experiments with the EDTA plasma. This could suggest that the contamination from the EDTA and citrate plasma contained differing levels of lipids and other biomolecules interfering with the protein assays [35,36], in turn suggesting the overall composition and characteristics of the contamination from the two types of plasma to differ. This point was confirmed using DLS, TEM, and LC-MS/MS, see Figure 2F-H: The contamination from the citrate plasma was found to contain smaller and more monodisperse particles than that from the EDTA plasma, but even more interesting, the contamination from the citrate plasma was found to be largely devoid of cytoskeleton proteins. Instead, apolipoproteins were found to represent >60% of the total protein in the contamination, apolipoprotein B alone representing ~25%. This may imply that the contamination contained a high abundance of lipoproteins [37]. On the other hand, the fact that the composition of the contamination changed completely upon changing the anticoagulant from EDTA to citrate suggests that at least one of the two anticoagulants engage in a complex set of interactions with both cells and various particles in the blood, forming distinct contaminant particles. Although the effect of the anticoagulant on the plasma proteome, metabolome, and lipidome is currently an active field of research [38], the mechanisms underlying our observations are not understood, yet it is clear that the role played by the anticoagulant goes beyond its primary mode of action, as both EDTA and citrate are known to exert their main anticoagulation effect by chelating calcium [39]. In any case, the proteomic content in the void volume for the citrate plasma was similar in the absence and presence of liposomes, see Figure S6B. Since it is unlikely that the liposomes were surrounded by a protein corona of the same protein composition as the contamination, the ~40% increase in the protein from the citrate plasma in the void volume induced by the liposomes was likely related to an increased level of contamination. The underlying mechanism of this effect is not understood, but could possibly have to do with the liposomes blocking the gel material from adsorbing the contaminant proteins and particles.

In addition to EDTA and citrate, heparin is a third commonly used type of anticoagulant [39]. This anticoagulant, however, may be inappropriate for protein corona studies as it interacts with several plasma proteins [40,41], potentially affecting their subsequent interactions with liposomes. Moreover, if the liposomes are positively charged, heparin may electrostatically adsorb to the liposomes and, thereby, alter their surface properties [42]. For completeness, though, we still investigated the magnitude of the protein contamination in the Sepharose CL-4B void volume for heparin plasma (see Figure S9 in the Supplementary material), finding it to be similar to that of EDTA

and citrate plasma. Due to the abovementioned reasons, however, we did not perform any additional studies with heparin plasma.

Having found that the contamination issue persists regardless of the choice of anticoagulant, we next considered whether extended centrifugation of the plasma prior to SEC would remove the contamination. To be more specific, the plasma used for the experiments described above was prepared with a standard centrifugation protocol, that is, the blood was centrifuged at 2,000 × *g* for 15 min. In addition to this, we now added an extended centrifugation step of 12,100 × *g* for 30 min before adding the liposomes to the plasma and running the SEC experiments as described above. We first tested the extended centrifugation protocol on EDTA plasma. For this type of plasma, the extended centrifugation did not lead to any detectable change in the total amount of protein in the plasma (see Figure S10 in the Supplementary material), yet the recorded protein elution profiles did not display any distinct protein peak in the void volume and were thus markedly different from

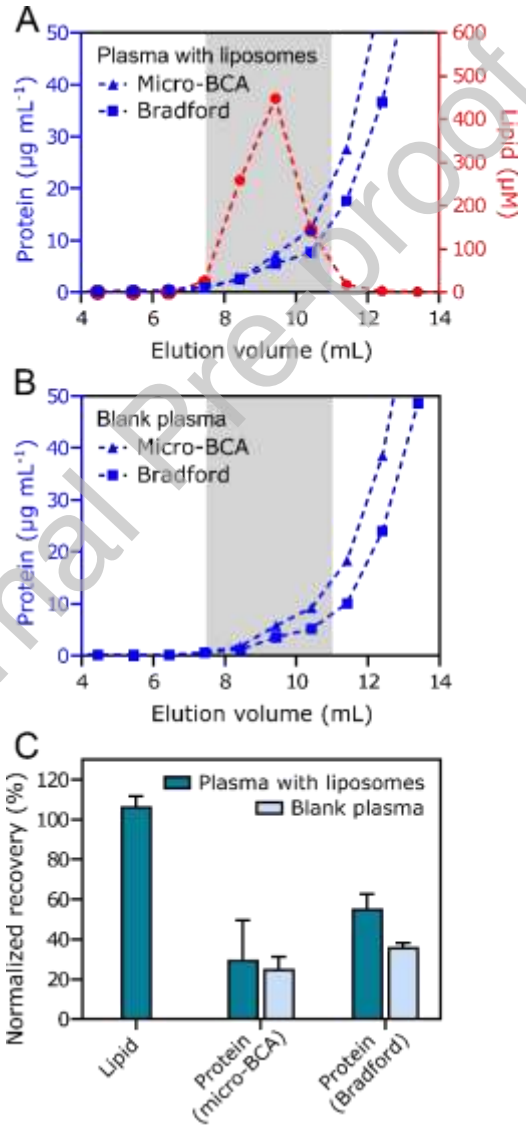

those of the standard EDTA plasma, see Figure 3A,B. This implies that contaminant particles were specifically removed from the plasma by the extended centrifugation protocol. In agreement with

Figure 3. Experiment with EDTA plasma prepared by an extended centrifugation protocol before being run on a 1.5×20-cm Sepharose CL-4B column. (A,B) Elution profiles in the vicinity of the void volume for plasma incubated with liposomes (A) or without liposomes (B). The shaded areas show the void volume. (C) Lipid and protein recovered in the void volume normalized to the amount recovered for EDTA plasma from the same donor prepared by a standard protocol. Panels A and B show example data from one sample, and Panel C shows the average data of two (plasma with liposomes) or three (blank plasma) separate sample pairs. The error bars represent the standard deviation.

this, we calculated that there was a 40-70% reduction of the protein content in the void volume compared to the standard EDTA plasma, no matter whether the plasma had been incubated with liposomes or not, see Figure 3C.

The shape of the elution profiles of the EDTA plasma prepared by the extended centrifugation protocol suggested that the protein remaining in the void volume represented a fronting region of the bulk protein peak. To investigate whether this was the case, we repeated the experiments with the centrifuged EDTA plasma using a longer, 1.5×50-cm Sepharose CL-4B column. Doing this, we almost completely removed the residual protein material in the void volume, both for plasma with and without liposomes, see Figure 4. Thus, removing protein contaminant particles from the plasma by centrifugation and using a longer Sepharose CL-4B column to avoid fronting effects sufficed to greatly reduce the contamination.

We next investigated the effect of subjecting citrate plasma to the extended centrifugation, but for this type of plasma, the protein elution profiles and the contamination level in the void volume of the 1.5×20-cm Sepharose CL-4B column remained largely unaffected by the centrifugation (see Figure S11 in the Supplementary material). This demonstrates that the extended centrifugation protocol is not universally applicable to reduce the contamination level in the void volume for all types of plasma.

To sum up, we found that a standard-size Sepharose CL-4B SEC column normally used for isolating liposomes is highly prone to protein contamination, but also that the contamination may be greatly reduced by using EDTA plasma prepared by an extended centrifugation protocol and a longer-than-standard Sepharose CL-4B column. Worth highlighting, with the exception of the centrifuged EDTA plasma, the contamination contained various particles of a similar size to the liposomes. Such

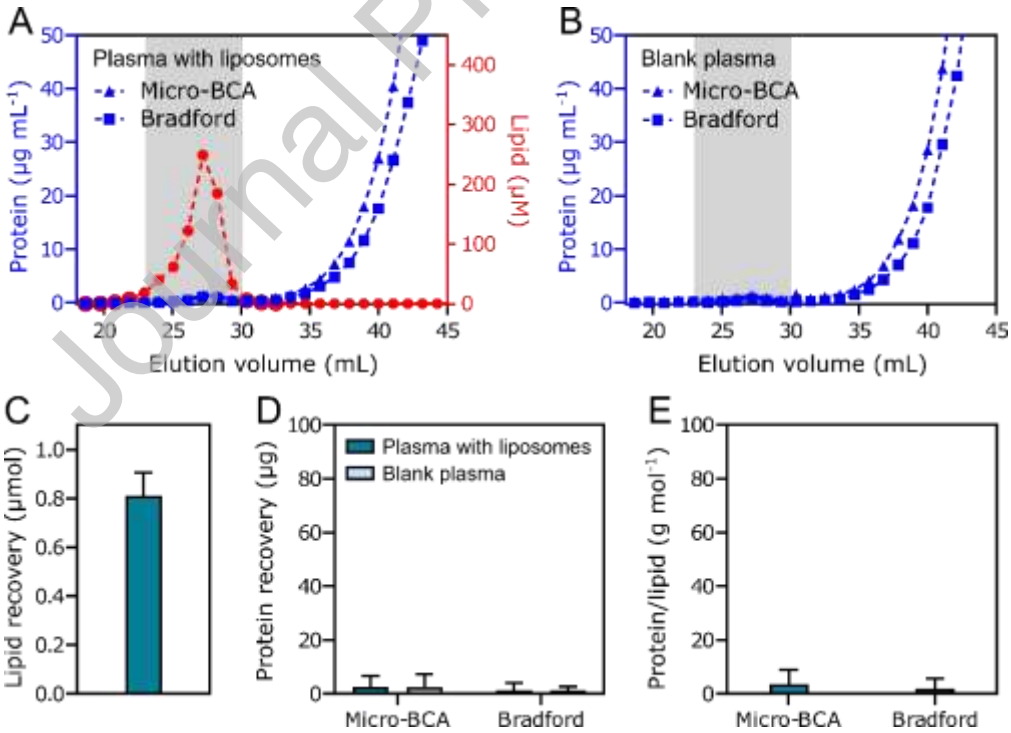

particles can, in principle, not be removed by any size-based isolation methods. Supporting this notion, protein particle contamination in the void volume was also reported in another recent study

Figure 4. Experiment with EDTA plasma prepared by an extended centrifugation protocol before being run on a 1.5×50-cm Sepharose CL-4B column. (A,B) Elution profiles in the vicinity of the void volume for plasma incubated with liposomes (A) or without liposomes (B). The shaded areas show the void volume. (C) Lipid recovered in the void volume for plasma incubated with liposomes. (D) Protein recovered in the void volume for both plasma incubated with or without liposomes. (E) Protein-to-lipid ratio in the void volume for plasma incubated with liposomes. Panels A and B show example data from one sample; and Panels C-E show the average data of two separate samples. The error bars

with human serum run on a Sepharose CL-4B column [13].

3.3. Isolation of liposomes using SEC in combination with membrane ultrafiltration

A number of recent studies have subjected liposomes recovered from serum or plasma by SEC to an additional membrane ultrafiltration step [12,13,15-17,19-21]. The purpose of this step has been to remove large proteins and protein aggregates, and concentrate the samples for improved downstream analysis. To investigate this approach, we repeated the experiments with standard EDTA and citrate plasma with and without liposomes run on the 1.5×20 cm Sepharose CL-4B column, but this time, the void-volume fractions were pooled and further subject to membrane ultrafiltration, first by a Vivaspin 6 filter unit (10,000 MW cut-off) and then by a Vivaspin 500 filter unit (1,000,000 MW cut-off), thereby following a protocol similar to one previously used [12,15-17,19,20].

Figure 5 shows the percentage of lipid and protein recovered in the membrane ultrafiltration step. Only a low percentage of protein was recovered in the experiments with the blank plasma, that is, most of the protein recovered from SEC was removed by the membrane ultrafiltration step. In contrast, a high percentage of protein and lipid was recovered in the experiments with the plasma with liposomes. From this, it might at first seem reasonable to assert that the membrane ultrafiltration step yielded a high liposome recovery and revealed the existence of a protein corona on the liposomes. However, whereas the interpretation about the high liposome recovery may be correct, an additional experiment revealed that the interpretation regarding the protein corona is not: Taking the void-volume eluate from a SEC run with blank plasma, and adding liposomes before subjecting the eluate to the membrane ultrafiltration step gave a similar level of lipid and protein recovery as in the experiments in which the plasma was mixed with liposomes before the SEC run. This demonstrates that the liposomes increased the recovery of the contaminant proteins in the membrane ultrafiltration step, in turn implying that the protein recovered from the plasma samples with liposomes should be ascribed to contamination. The mechanism underlying the increase in contamination induced by the liposomes is not understood, but as suggested for the SEC experiments with the citrate plasma, it could have to do with the liposomes blocking the filter material from adsorbing the contaminant proteins and particles. No matter the explanation, though, it seems that the combined SEC/membrane ultrafiltration method may be no less prone to protein contamination than SEC alone, and in addition, it suffers to a much higher extent from the challenge

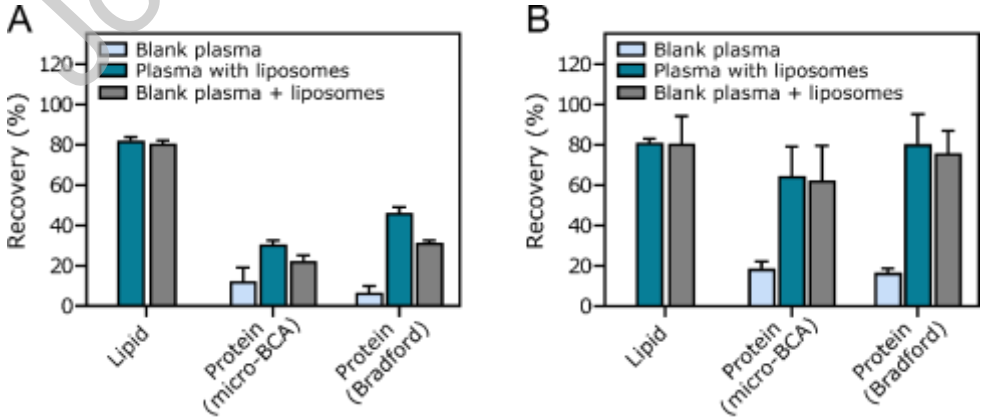

that it does not allow for a blank control experiment to reveal the contamination recovered together with the liposomes, that is, running a blank plasma sample does not provide a representation of the

Figure 5. Experiment with plasma run on a 1.5×20-cm Sepharose CL-4B column and subsequent membrane ultrafiltration of the void-volume eluate. (A,B) Lipid and protein recovered in the membrane ultrafiltration step for samples from EDTA plasma (A) or citrate plasma (B) incubated with or without liposomes. As an additional experiment, liposomes were added to the void-volume eluate of blank plasma before performing the membrane ultrafiltration step. The data are the average of two (all data except for blank EDTA plasma) or three (blank EDTA plasma) separate samples, and the error bars represent the standard deviation.

protein contamination recovered from plasma samples with liposomes. From that point of view, it seems recommendable to use SEC alone to recover the liposomes rather than adding an additional membrane ultrafiltration step.

3.4. Isolation of liposomes using centrifugation

Many studies on the liposomal protein corona are based on centrifugation as the isolation method [29-31,43-48]. In light of its widespread usage, we also wanted to investigate the efficiency of this method.

The basic concept of the centrifugation isolation method is to subject liposomes in serum/plasma to a centrifugal force that will cause them to sediment together with any proteins bound to their surface. To test the method, we incubated stealth liposomes in standard EDTA plasma–as described above–and subsequently, we subjected the samples to centrifugation for 30 min at 17,900 × *g*, almost the highest g-force tolerated by the Protein LoBind tubes containing the samples. Following this procedure, however, we encountered a severe obstacle that prompted us to halt further work: The liposomes did not sediment, see Figure 6. Demonstrating that we are not the only ones to have this issue, another recent study reported the exact same thing [49]. Given the popularity of the centrifugation isolation method, the lacking sedimentation of the liposomes may seem surprising, but considering the theory of centrifugation, it is actually not. The centrifugal sedimentation rate of any given object is linearly proportional to the difference between the density of the object and the surrounding medium, and since empty unilamellar liposomes are of a similar density to plasma–both primarily consist of water–it is apparent that it may be very difficult to sediment the liposomes, and not even higher centrifugation speeds would necessarily solve the problem. A potential strategy to mitigate the problem, though, could be to increase the density of the liposomes. This could, for instance, be achieved by loading the liposomes with the drug doxorubicin, which upon entering the inner lumen of the liposomes form crystalline structures [50,51].

Resolving the problem with lacking liposome sedimentation is beyond the scope of the present study, yet it is still of interest to contemplate whether the centrifugation method may potentially also suffer from protein contamination. Suggesting that this is the case, some centrifugation-based studies have as part of the liposomal protein corona identified many of the exact same proteins–including some of the cytoskeleton proteins–that we found to be associated with the particles that sedimented from EDTA plasma during the centrifugation at 12,100 × *g* described above [43,45]. Further adding to the risk of contamination, both serum and plasma contains a very high amount of soluble protein, and even if just a minute amount of this protein is recovered with the liposomes, it will represent a significant source of contamination. Supporting this notion, it was recently demonstrated that considerable amounts of serum albumin–the most abundant protein in serum and plasma–was sedimented from serum at centrifugation speeds at which liposomes still remained

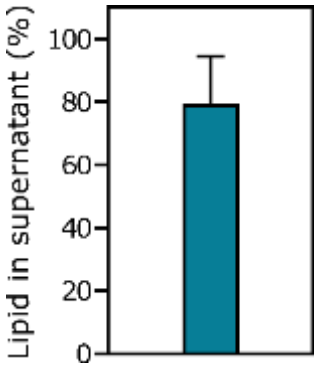

Figure 6. Percentage lipid remaining in the supernatant upon centrifugation of EDTA plasma with liposomes for 30 min at 17,900 × g. The data are the average of three separate samples, and the error bars represent the standard deviation.

in suspension [49]. Thus, even if the problem of lacking liposome sedimentation is solved, the issue of protein contamination may still impact studies using centrifugation as the liposome isolation method.

3.5. Implications of the contamination issue on the liposome-protein corona research field

From the data presented above, it is clear that protein contamination may represent an issue for studies on the protein corona on stealth liposomes when using standard liposome isolation methods. This naturally raises the question of whether contamination may also impact studies on other types of liposomes. To approach this question, consider that we recovered a protein-to-lipid ratio in the range 20-80 g protein per mol lipid for the stealth liposomes when using standard size-based isolation methods. Since the protein corona of stealth liposomes was found to be negligible, this ratio represents the protein contamination-to-lipid ratio, implying that the protein binding value of any given type of liposome has to be much higher than this ratio for the protein contamination to be ignored in the data analysis. If the study is performed using a lower liposome concentration, the reference protein contamination-to-lipid ratio would be even higher, see Figure S12 in the Supplementary material. Going through the literature, the protein binding value is often reported to be <100 g protein per mol lipid for a variety of different types of liposomes [7-11,14,18,21]. This implies that protein contamination may generally impact studies on the liposomal protein corona, at least if the studies are based on standard plasma and isolation methods. However, for certain non-PEGylated cationic liposomes, the protein binding value may be ≫100 g protein per mol lipid [8,52], indicating that the protein contamination is of lesser importance when studying such liposomes.

Evidently, if the contamination is reduced, its impact on the data analysis will decrease. Therefore, it is interesting that we found the contamination to be greatly reduced by subjecting EDTA plasma to extended centrifugation and then using a longer-than-standard Sepharose CL-4B column to isolate the liposomes. This strategy seems promising, although it should be mentioned that it comes with the risk of omitting plasma components–such as certain lipoproteins–that potentially may interact with the liposomes [53]. The same point also applies when removing contaminant particles using size-based methods [13]. Therefore, it is still of interest to the field to develop more advanced liposome isolation methods, for example, based on using specific molecules on the surface of the liposomes for affinity chromatography [54,55], on immobilizing the liposomes on a surface [56], or on cross-linking of proteins in the corona to the liposomal lipids [49].

In any case, it is advisable that all studies on the liposomal protein corona include a control experiment to estimate the protein contamination recovered with the liposomes. This point is not as trivial as it may sound: We have here shown that when using a Sepharose CL-4B column to isolate liposomes, running a blank plasma sample provides a reasonable representation of the contamination recovered together with the liposomes from plasma. However, when using the same column in combination with membrane ultrafiltration, running a blank plasma sample does not provide an accurate description of the contamination recovered with the liposomes. Without this information, it is impossible to assess which proteins should be ascribed to the protein corona and which proteins should be ascribed to the contamination.

Unfortunately, the far majority of the studies on the liposomal protein corona cited above do not report a blank control experiment to assess the contamination recovered with the liposomes, that is, either the studies do not report a blank control experiment at all, or they employ the combined SEC/membrane ultrafiltration method, which does not allow for a complete assessment of the contaminant proteins recovered with the liposomes. It is evident that this lack of proper control

experiments may represent a fundamental issue for the liposome-protein corona research field, in worst case even representing the core reason for the widespread confusion about the nature of the liposomal protein corona. Whether or not this is the case, it is clear that future studies on the liposomal protein corona should make a virtue of appropriately performing and reporting their control experiments.

For completeness, it should be mentioned that the above considerations do not only apply to studies on the liposomal protein corona; they may equally well apply to studies on the protein corona of other nanomaterials. Supporting this point, protein contamination has been found to impact studies on the protein corona of polystyrene nanoparticles [57] and various other polymer nanoparticles [25]. This highlights that the protein corona field as a whole is in need of a standardized set of working guidelines [58]. The work that we have presented here help to concretize how to formulate such guidelines, specifically by describing the efficiency of commonly used isolation methods.

3.6. A general limitation for all isolation methods

The above work focused on how to study the liposomal protein corona using isolation methods, so a final, general point about the usage of such methods should be made: Like the protein corona on other nanomaterials, the protein corona on liposomes is principally comprised of two components, namely the hard and the soft corona [59,60]. The hard corona represents proteins that are tightly bound to the liposomes, that is, proteins that remain bound to the liposomes during isolation from serum/plasma. The soft corona represents more loosely bound proteins that dissociate from the liposomes during the isolation. It has been suggested that by using particularly mild isolation methods, it is also possible to probe the soft corona [61], but assuming this component of the corona to represent a dynamic equilibrium [62-64], this is conceptually incorrect: Any isolation step decreasing the protein concentration in the vicinity of the liposomes will shift the surface binding equilibrium towards dissociated proteins and thereby lead to removal of loosely bound proteins, no matter the external physical forces exerted on the system. When using isolated liposomes for characterizing the protein corona, it is thus an inherent premise that only information about the hard corona is obtainable [65,66]. This limitation applies to all known isolation methods, and at present, there exist no conceptual strategies to overcome it. Upon obtaining a converging understanding about the hard protein corona on liposomes, one of the next aims of the liposome-protein corona research field may thus be to develop approaches to understand how the hard protein corona relates to the *in situ* protein corona on liposomes circulating in the bloodstream.

4. Conclusion

We have demonstrated that protein contamination represents a significant challenge when isolating stealth liposomes from human plasma using a standard SEC method alone or in combination with membrane ultrafiltration. In addition, we have shown that centrifugation does not readily sediment the liposomes, and we have argued that this method may also be susceptible to protein contamination. It seems that these issue have not been taken into account in previous studies on the liposomal protein corona, representing a potential reason why the studies reach contradicting conclusions.

Declaration of interests

☒ The authors declare that they have no known competing financial interests or personal relationships that could have appeared to influence the work reported in this paper.

☐The authors declare the following financial interests/personal relationships which may be considered as potential competing interests:

Acknowledgements

The authors thank Anne Z. Eriksen and Katrine Jønsson for drawing the blood samples, and Fredrik Melander and Gael C. Veiga for performing the ICP-MS recordings. Financial support for this work was kindly provided by the Lundbeck Foundation (grant no. R155-2013-14113) and the Novo Nordisk Foundation (grant no. NNF16OC0022166). Additional funding for the LC-MS/MS experiments was provided by the Danish Agency for Science and Higher Education (grant no. 5072-00007B), the Obelske Family Foundation, the Svend Andersen Foundation, and the Spar Nord Foundation.

References

1. T.M. Allen, P.R. Cullis, Liposomal drug delivery systems: from concept to clinical applications, Adv. Drug Deliv. Rev. 65 (2013) 36-48.
2. U. Bulbake, S. Doppalapudi, N. Kommineni, W. Khan, Liposomal formulations in clinical use: an updated review, Pharmaceutics 9 (2017) 12.
3. L. Sercombe, T. Veerati. F. Moheimani, S.Y. Wu, A.K. Sood, S. Hua, Advances and challenges of liposome assisted drug delivery, Front. Pharmacol. 6 (2015) 286.
4. G. Caracciolo, Liposome-protein corona in a physiological environment: challenges and opportunities for targeted delivery of nanomedicines, Nanomedicine 11 (2015) 543-557.
5. M.L. Immordino, F. Dosio, L. Cattel, Stealth liposomes: review of the basic science, rationale, and clinical applications, existing and potential, Int. J. Nanomedicine 1 (2006) 297-315.
6. P. Jain, R.S. Pawar, R.S. Pandey, J. Madan, S. Pawar, P.K. Lakshmi, M.S. Sudheesh, In-vitro in-vivo correlation (IVIVC) in nanomedicine: is protein corona the missing link?, Biotechnol. Adv. 35 (2017) 889-904.
7. A. Chonn, S.C. Semple, P.R. Cullis, Association of blood proteins with large unilamellar liposomes in vivo. Relation to circulation lifetimes, J. Biol. Chem. 267 (1992) 18759-18765.
8. S.C. Semple, A. Chonn, P.R. Cullis, Interactions of liposomes and lipid-based carrier systems with blood proteins: Relation to clearance behaviour in vivo, Adv. Drug Deliv. Rev. 32 (1998) 3-17.
9. S.C. Semple, A. Chonn, P.R. Cullis, Influence of cholesterol on the association of plasma proteins with liposomes, Biochemistry 35 (1996) 2521-2525.
10. S.A. Johnstone, D. Masin, L. Mayer, M.B. Bally, Surface-associated serum proteins inhibit the uptake of phosphatidylserine and poly(ethylene glycol) liposomes by mouse macrophages, Biochim. Biophys. Acta 1513 (2001) 25-37.
11. N. Dos Santos, C. Allen, A.-M. Doppen, M. Anantha, K.A.K. Cox, R.C. Gallagher, G. Karlsson, K. Edwards, G. Kenner, L. Samuels, M.S. Webb, M.B. Bally, Influence of poly(ethylene glycol) grafting density and polymer length on liposomes: relating plasma circulation lifetimes to protein binding, Biochim. Biophys. Acta 1768 (2007) 1367-1377.
12. M. Hadjidemetriou, Z. Al-Ahmady, M. Mazza, R.F. Collins, K. Dawson, K. Kostarelos, In vivo biomolecule corona around blood-circulating, clinically used and antibody-targeted lipid bilayer nanoscale vesicles, ACS Nano 9 (2015) 8142-8156.
13. K. Yang, B. Mesquita, P. Horvatovich, A. Salvati, Tuning liposome composition to modulate corona formation in human serum and cellular uptake, Acta Biomater. 106 (2020) 314-327.
14. T. Ishida, M. Ichihara, X.Y. Wang, K. Yamamoto, J. Kimura, E. Majima, H. Kiwada, Injection of PEGylated liposomes in rats elicits PEG-specific IgM, which is responsible for rapid elimination of a second dose of PEGylated liposomes, J. Control. Release 112 (2006) 15-25.
15. M. Hadjidemetriou, Z. Al-Ahmady, K. Kostarelos, Time-evolution of in vivo protein corona onto blood-circulating PEGylated liposomal doxorubicin (DOXIL) nanoparticles, Nanoscale 8 (2016) 6948-6957.
16. M. Hadjidemetriou, S. McAdam, G. Garner, C. Thackeray, D. Knight, D. Smith, Z. Al-Ahmady, M. Mazza, J. Rogan, A. Clamp, K. Kostarelos, The human in vivo biomolecule corona onto PEGylated liposomes: a proof-of-concept clinical study, Adv. Mater. 31 (2019) e1803335.
17. M. Hadjidemetriou, J. Rivers-Auty, L. Papafilippou, J. Eales, K.A.B. Kellett, N.H. Hooper, C.B. Lawrence, K. Kostarelos, Nanoparticle-enabled enrichment of longitudinal blood proteomic fingerprints in Alzheimer's disease, ACS Nano 15 (2021) 7357-7369.

18. K. Kristensen, T.B. Engel, A. Stensballe, J.B. Simonsen, T.L. Andresen, The hard protein corona of stealth liposomes is sparse, J. Control. Release 307 (2019) 1-15.
19. Z.S. Al-Ahmady, M. Hadjidemetriou, J. Gubbins, K. Kostarelos, Formation of protein corona in vivo affects drug release from temperature-sensitive liposomes, J. Control. Release 276 (2018) 157-167.
20. L. Papafilippou, A. Claxton, P. Dark, K. Kostarelos, M. Hadjidemetriou, Protein corona fingerprinting to differentiate sepsis from non-infectious systemic inflammation, Nanoscale 12 (2020) 10240-10253.
21. W.J.M. Lokerse, A. Lazarian, A. Kleinhempel, M. Petrini, P. Schwarz, M. Hossann, L.M. Holdt ,V. Mailänder, L.H. Lindner, Mechanistic investigation of thermosensitive liposome immunogenicity and understanding the drivers for circulation half-life: A polyethylene glycol versus 1,2-dipalmitoyl-sn-glycero-3-phosphodiglycerol study, J. Control. Release 333 (2021) 1-15.
22. J. Cox, M. Mann, MaxQuant enables high peptide identification rates, individualized p.p.b.-range mass accuracies and proteome-wide protein quantification, Nat. Biotechnol. 26 (2008) 1367-1372.
23. S. Tyanova, T. Temu, P. Sinitcyn, A. Carlson, M.Y. Hein, T. Geiger, M. Mann, J. Cox, The Perseus computational platform for comprehensive analysis of (prote)omics data, Nat. Methods 13 (2016) 731-740.
24. L. Hagel, M. Östberg, T. Andersson, Apparent pore size distributions of chromatography media, J. Chromatogr. A 743 (1996) 33-42.
25. I. Alberg, S. Kramer, M. Schinnerer, Q. Hu, C. Seidl, C. Leps, N. Drude, D. Möckel, C. Rijcken, T. Lammers, M. Diken, M. Maskos, S. Morsbach, K. Landfester, S. Tenzer, M. Barz, R. Zentel, Polymeric nanoparticles with neglectable protein corona, Small 16 (2020) e1907574.
26. R. Münter, K. Kristensen, D. Pedersbæk, J.B. Larsen, J.B. Simonsen, T.L. Andresen, Dissociation of fluorescently labeled lipids from liposomes in biological environments challenges the interpretation of uptake studies, Nanoscale 10 (2018) 22720-22724.
27. F.A.W. Coumans, A.R. Brisson, E.I. Buzas, F. Dignat-George, E.E.E. Drees, S. El-Andaloussi, C. Emanueli, A. Gasecka, A. Hendrix, A.F. Hill, R. Lacroix, Y. Lee, T.G. van Leeuwen, N. Mackman, I. Mäger, J.P. Nolan, E. van der Pol, D.M. Pegtel, S. Sahoo, P.R.M. Siljander, G. Sturk, O. de Wever, R. Nieuwland, Methodological guidelines to study extracellular vesicles, Circ. Res. 120 (2017) 1632-1648.
28. G. van Niel, G. D'Angelo, G. Raposo, Shedding light on the cell biology of extracellular vesicles, Nat. Rev. Mol. Cell Biol. 19 (2018) 213-228.
29. A.L. Capriotti, G. Caracciolo, C. Cavaliere, P. Foglia, D. Pozzi, R. Samperi, A. Laganà, Do plasma proteins distinguish between liposomes of varying charge density?, J. Proteomics 75 (2012) 1924-1932.
30. G. Caracciolo, D. Pozzi, A.L. Capriotti, C. Cavaliere, S. Piovesana, G. La Barbera, A. Amici, A. Laganà, The liposome-protein corona in mice and humans and its implications for in vivo delivery, J. Mater. Chem. B 2 (2014) 7419-7428.
31. V.P. Vu, G.B. Gifford, F. Chen, H. Benasutti, G. Wang, E.V. Groman, R. Scheinman, L. Saba, S.M. Moghimi, D. Simberg, Immunoglobulin deposition on biomolecule corona determines complement opsonization efficiency of preclinical and clinical nanoparticles, Nat. Nanotechnol. 14 (2019) 260-268.
32. S. Tenzer, D. Docter, J. Kuharev, A. Musyanovych, V. Fetz, R. Hecht, F. Schlenk, D. Fischer, K. Kiouptsi, C. Reinhardt, K. Landfester, H. Schild, M. Maskos, S.K. Knauer, R.H. Stauber, Rapid

formation of plasma protein corona critically affects nanoparticle pathophysiology, Nat. Nanotechnol. 8 (2013) 772-781.

33. S. Schöttler, K. Klein, K. Landfester, V. Mailänder, Protein source and choice of anticoagulant decisively affect nanoparticle protein corona and cellular uptake, Nanoscale 8 (2016) 5526-5536.
34. M. Lundqvist, C. Augustsson, M. Lilja, K. Lundkvist, B. Dahlbäck, S. Linse, T. Cedervall, The nanoparticle protein corona formed in human blood or human blood fractions, PLoS ONE 12 (2017) e0175871.
35. R.J. Kessler, D.D. Fanestil, Interference by lipids in the determination of protein using bicinchoninic acid, Anal. Biochem. 159 (1986) 138-142.
36. R.E. Morton, T.A. Evans, Modification of the bicinchoninic acid protein assay to eliminate lipid interference in determining lipoprotein protein content, Anal. Biochem, 204 (1992) 332-334.
37. J.B. Simonsen, R. Münter, Pay attention to biological nanoparticles when studying the protein corona on nanomedicines, Angew. Chem. Int. Ed. Engl. 59 (2020) 12584-12588.
38. M. Khadka, A. Todor, K.M. Maner-Smith, J.K. Colucci, V. Tran, D.A. Gaul, E.J. Anderson, M.S. Natrajan, N. Rouphael, M.J. Mulligan, C.E. McDonald, M. Suthar, S. Li, E. A. Ortlund, The effect of anticoagulants, temperature, and time on the human plasma metabolome and lipidome from healthy donors as determined by liquid chromatography-mass spectrometry, Biomolecules 9 (2019) 200.
39. E. Cedrone, B.W. Neun, J. Rodriguez, A. Vermilya, J.D. Clogston, S.E. McNeil, Y. Barenholz, J. Szebeni, M.A. Dobrovolskaia, Anticoagulants influence the performance of in vitro assays intended for characterization of nanotechnology-based formulations, Molecules 23 (2018) 12.
40. I. Capila, R.J. Linhardt, Heparin-protein interactions, Angew. Chem. Int. Ed. Engl. 41 (2002) 391-412.
41. G. Berrecoso, J. Crecente-Campo, M.J. Alonso, Unveiling the pitfalls of the protein corona of polymeric drug nanocarriers, Drug Deliv. Transl. Res. 10 (2020) 730-750.
42. J. Marques, E. Moles, P. Urbán, R. Prohens, M.A. Busquets, C. Sevrin, C. Grandfils, X. Fernàndez-Busquets, Application of heparin as a dual agent with antimalarial and liposome targeting activities toward Plasmodium-infected red blood cells, Nanomedicine 10 (2014) 1719-1728.
43. A.L. Barrán-Berdón, D. Pozzi, G. Caracciolo, A.L. Cappriotti, G. Caruso, C. Cavaliere, A. Riccioli, S. Palchetti, A. Laganà, Time evolution of nanoparticle-protein corona in human plasma: relevance for targeted drug delivery, Langmuir 29 (2013) 6485-6494.
44. A. Bigdeli, S. Palchetti, D. Pozzi, M.R. Hormozi-Nezhad, F.B. Bombelli, G. Caracciolo, M. Mahmoudi, Exploring cellular interactions of liposomes using protein corona fingerprints and physicochemical properties, ACS Nano 10 (2016) 3723-3737.
45. C. Corbo, R. Molinaro, F. Taraballi, N.E.T. Furman, K.A. Hartman, M.B. Sherman, E. De Rosa, D.K. Kirui, F. Salvatore, E. Tasciotti, Unveiling the in vivo protein corona of circulating leukocyte-like carriers, ACS Nano 11 (2017) 3262-3273.
46. M. Papi, D. Caputo, V. Palmieri, R. Coppola, S. Palchetti, F. Bugli, C. Martini, L. Digiacomo, D. Pozzi, G. Caracciolo, Clinically approved PEGylated nanoparticles are covered by a protein corona that boosts the uptake by cancer cells, Nanoscale 9 (2017) 10327-10334.
47. G. Caracciolo, S. Palchetti, L. Digiacomo, R.Z.Z. Chiozzi, A.L. Capriotti, H. Amenitsch, P.M. Tentori, V. Palmieri, M. Papi, F. Cardarelli, D. Pozzi, A. Laganà, Human biomolecular corona of liposomal doxorubicin: the overlooked factor in anticancer drug delivery, ACS Appl. Mater. Interfaces 10 (2018) 22951-22962.

48. F. Giulimondi, L. Digiacomo, D. Pozzi, S. Palchetti, E. Vulpis, A.L. Cappriotti, R.Z. Chiozzi, A. Laganà, H. Amenitsch, L. Masuelli, G. Peruzzi, M. Mahmoudi, I. Screpanti, A. Zingoni, G. Caracciolo, Interplay of protein corona and immune cells controls blood residency of liposomes, Nat. Commun. 10 (2019) 3686.
49. R. Pattipeiluhu, S. Crielaard, I. Klein-Schiphorst, B.I. Florea, A. Kros, F. Campbell, Unbiased identification of the liposome protein corona using photoaffinity-based chemoproteomics, ACS Cent. Sci. 6 (2020) 535-545.
50. Y. Barenholz, Doxil® – the first FDA-approved nano-drug: lessons learned, J. Control. Release 160 (2012) 117-134.
51. D. Mehn, P. Iavicoli, N. Cabaleiro, S.E. Borgos, F. Caputo, O. Geiss, L. Calzolai, F. Rossi, D. Gilliland, Analytical ultracentrifugation for analysis of doxorubicin loaded liposomes, Int. J. Pharm. 523 (2017) 320-326.
52. N. Oku, Y. Tokudome, Y. Namba, N. Saito, M. Endo, Y. Hasegawa, M. Kawai, H. Tsukada, S. Okada, Effect of serum protein binding on real-time trafficking of liposomes with different charges analyzed by positron emission tomography, Biochim. Biophys. Acta 1280 (1996) 149-154.
53. A. Akinc, W. Querbes, S. De, J. Qin, M. Frank-Kamenetsky, K.N. Jayaprakash, M. Jayaraman, K.G. Rajeev, W.L. Cantley, J.R. Dorkin, J.S. Butler, L. Qin, T. Racie, A. Sprague, E. Fava, A. Zeigerer, M.J. Hope, M. Zerial, D.W.Y. Sah, K. Fitzgerald, M.A. Tracy, M. Manoharan, V. Koteliansky, A. de Fougerolles, M.A. Maier, Targeted delivery of RNAi therapeutics with endogenous and exogenous ligand-based mechanisms, Mol. Ther. 18 (2010) 1357-1364.
54. R.C. Lai, K.H. Tan, S.K. Lim, Membrane lipid binding molecules for the isolation of bona fide extracellular vesicle types and associated biomarkers in liquid biopsy, J. Cancer Metastasis Treat. 5 (2019) 65.
55. Y. Chu, W. Tang, Z. Zhang, C. Li, J. Qian, X. Wei, T. Ying, W. Lu, C. Zhan, Deciphering protein corona by scFv-based affinity chromatography, Nano Lett. 21 (2021) 2124-2131.
56. O.K. Kari, J. Ndika, P. Parkkila, A. Louna, T. Lajunen, A. Puustinen, T. Viitala, H. Alenius, A. Urtti, In situ analysis of liposome hard and soft protein corona structure and composition in a single label-free workflow, Nanoscale 12 (2020) 1728-1741.
57. S. Sheibani, K. Basu, A. Farnudi, A. Ashkarran, M. Ichikawa, J.F. Presley, K.H. Bui, M.R. Ejtehadi, H. Vali, M. Mahmoudi, Nanoscale characterization of the biomolecular corona by cryo-electron microscopy, cryo-electron tomography, and image simulation, Nat. Commun. 12 (2021) 573.
58. A.J. Chetwynd, K.E. Wheeler, I. Lynch, Best practice in reporting corona studies: Minimum information about Nanomaterial Biocorona Experiments (MINBE), Nano Today 28 (2019) 100758.
59. D. Docter, D. Westmeier, M. Markiewicz, S. Stolte, S.K. Knauer, R.H. Stauber, The nanoparticle biomolecule corona: lessons learned – challenge accepted? Chem. Soc. Rev. 44 (2015) 6094-6121.
60. R. García-Álvarez, M. Vallet-Regí, Hard and soft protein corona of nanomaterials: Analysis and relevance, Nanomaterials 11 (2021) 888.
61. C. Weber, M. Voigt, J. Simon, A.-K. Danner, H. Frey, V. Mailänder, M. Helm, S. Morsbach, K. Landfester, Functionalization of liposomes with hydrophilic polymers results in macrophage uptake independent of the protein corona, Biomacromolecules 20 (2019) 2989-2999.

62. T. Cedervall, I. Lynch, S. Lindman, T. Berggård, E. Thulin, H. Nilsson, K.A. Dawson, S. Linse, Understanding the nanoparticle-protein corona using methods to quantify exchange rates and affinities of proteins for nanoparticles, Proc. Natl. Acad. Sci. USA 104 (2007) 2050-2055.
63. S. Milani, F.B. Bombelli, A.S. Pitek, K.A. Dawson, J. Rädler, Reversible versus irreversible binding of transferrin to polystyrene nanoparticles: soft and hard corona, ACS Nano 6 (2012) 2532-2541.
64. K. Kristensen, A.J. Urquhart, E. Thormann, T.L. Andresen, Binding of human serum albumin to PEGylated liposomes: insights into binding numbers and dynamics by fluorescence correlation spectroscopy, Nanoscale 8 (2016) 19726-19736.
65. D. Sanchez-Guzman, G. Giraudon-Colas, L. Marichal, Y. Boulard, F. Wien, J. Degrouard, A. Baeza-Squiban, S. Pin, J.P. Renault, S. Devineau, In situ analysis of weakly bound proteins reveals molecular basis of soft corona formation, ACS Nano 14 (2020) 9073-9088.
66. H. Mohammad-Beigi, Y. Hayashi, C.M. Zeuthen, H. Eskandari, C. Scavenius, K. Juul-Madsen, T. Vorup-Jensen, J.J. Enghild, D.S. Sutherland, Mapping and identification of soft corona proteins at nanoparticles and their impact on cellular association, Nat. Commun. 11 (2020) 4535.